

Core polarization effects in *sd*-shell nuclei and charge-symmetry breaking in the nuclear mean field

N. Auerbach

School of Physics and Astronomy, Tel Aviv University, Tel Aviv 69978, Israel

J. Bartel and G. Wenes

Theoretical Division, Los Alamos National Laboratory, Los Alamos, New Mexico 87545

(Received 11 July 1988)

The proton and neutron densities and nuclear potentials are calculated for the deformed *sd*-shell nuclei ^{28}Si and ^{32}S in the framework of the constrained Hartree-Fock method and compared with the results of the spherical nucleus ^{40}Ca . Coulomb core polarization effects are responsible for differences in the proton and neutron Hartree-Fock potentials. These charge-asymmetry effects in the nuclear mean field must be taken into account when trying to decide whether the charge asymmetry observed in proton and neutron scattering is due to a genuine charge asymmetry in the nuclear force and, if possible, to put an upper limit on the magnitude of this effect. Our calculations indicate that there is no enhancement of the charge asymmetry due to nuclear deformation. The often proposed volume integral of the nuclear potential is found not to be an appropriate tool to investigate charge-asymmetry effects in nuclei due to a large cancellation in the integral.

I. INTRODUCTION

Several very precise experiments of elastic scattering of neutrons on $N=Z$ nuclei were performed recently in order to study a charge asymmetry in the nucleon-nucleon interaction.¹⁻⁴ Through a comparison of these experiments with those performed by elastic proton scattering on the same nuclei, one hopes to be able to learn something about possible charge-symmetry violation in nuclei. In this comparison, however, one has to account for the effects of the Coulomb interaction of the protons in the target nucleus.

The choice of $N=Z$ nuclei as targets was made in order to have a symmetric situation as far as the nuclear force is concerned. Therefore, any asymmetry detected would indicate a charge asymmetry in the nuclear force. The comparison of the scattering of neutrons and protons on the same $N=Z$ target nucleus can be seen in complete analogy with, and an extension to, the comparison of the binding energies of two mirror nuclei, i.e., the determination of the Coulomb displacement energy (CDE).⁵ For example the comparison of the $p + ^{40}\text{Ca}$ and the $n + ^{40}\text{Ca}$ scattering is analogous to the CDE for the ^{41}Sc - ^{41}Ca isospin doublet. In the latter case one deals with the interaction of a bound proton and neutron with the ^{40}Ca core, while in the former case the proton and neutron are in an unbound state.

The theoretical attempts to calculate the CDE for conjugate nuclei such as the pair ^{41}Sc - ^{41}Ca have only been partly successful and a discrepancy still exists between theory and experiment, the experimental CDE exceeding the theoretical one⁵ by 4–5%. This discrepancy is referred to as the Nolen-Schiffer anomaly.⁶

In order to achieve very precise theoretical results for the CDE, one must perform calculations of higher-order Coulomb correction terms. These calculations are involved and often model dependent. In particular one

should mention here mixed second-order corrections which involve core polarization and which are of first order in the Coulomb interaction and of first order in the strong interaction.^{7,5} These core-polarization corrections can be viewed as a small symmetry potential in the $N=Z$ core (see Refs. 5, 7, and 8 for a detailed discussion). When we speak about *symmetry potential* we mean that part of the nuclear potential that results from the difference in the $T=0$ and $T=1$ parts of the n - p interaction. In the case of a $N=Z$ nucleus the symmetry potential is—due to the difference in the proton-neutron density—a charge-asymmetric potential. In order to avoid any confusion, we will speak about the just mentioned *symmetry potential* and about the *charge-asymmetric potential* caused by a different distribution of protons and neutrons in the nucleus.

When making the comparison between the proton and neutron scattering from $N=Z$ target nuclei, some of the higher-order effects considered in the case of the CDE should also be taken into account. Most definitely one must add the small symmetry potential resulting from the core polarization before any meaningful conclusions about the asymmetry in the nuclear force can be drawn from the scattering experiments. It is the purpose of this paper to calculate these polarization potentials for several nuclei and in particular for nuclei that are considered deformed. To our knowledge, this is the first time that such effects are analysed for deformed nuclei.

II. THE CHARGE-ASYMMETRIC CORE-POLARIZATION SYMMETRY POTENTIAL

The Coulomb interaction between protons tries to repel the protons from each other and displace them with respect to the neutrons, while the attractive nuclear force, and in particular the proton-neutron interaction, resists this tendency. As a result an equilibrium is

reached in $N=Z$ nuclei in which the proton density is only slightly expelled with respect to the neutron density.^{5,8,9}

In Fig. 1 we present an example of the difference in $\rho_p - \rho_n$ obtained for ^{40}Ca in the Hartree-Fock (HF) approach using the Skyrme SIII force.¹⁰ The difference in the proton and neutron rms radii is $\langle r_p^2 \rangle^{1/2} - \langle r_n^2 \rangle^{1/2} = 0.04$ fm, which is only about 1% of the ^{40}Ca radius. This difference is expected to give rise to a small symmetry potential. The density, when correlated with the strong nucleon-nucleon force, should lead to $U_1 \equiv U_p - U_n \neq 0$ where U_p and U_n are the self-consistent proton and neutron HF nuclear potentials (i.e., leaving out the Coulomb potential for the protons). Since the average n - p interaction (which contains the $T=0$ and $T=1$ parts) is more attractive than the p - p interaction, one should expect in the nuclear surface a more attractive potential for a neutron than for a proton. Our HF calculations for the spherical nuclei do indeed give a deeper negative potential for neutrons than protons. One can obtain this result explicitly using an interaction of the

Skyrme type^{11,12}

$$\begin{aligned} v(\mathbf{R}, \mathbf{s}) = & t_0(1+x_0 P_\sigma) \delta(\mathbf{s}) \\ & + \frac{t_1}{2}(1+x_1 P_\sigma) [\delta(\mathbf{s}) \mathbf{k}^2 + \mathbf{k}'^2 \delta(\mathbf{s})] \\ & + t_2(1+x_2 P_\sigma) \mathbf{k}' \cdot \delta(\mathbf{s}) \mathbf{k} \\ & + \frac{t_3}{6}(1+x_3 P_\sigma) \rho^\alpha(\mathbf{R}) \delta(\mathbf{s}), \end{aligned} \quad (1)$$

where \mathbf{s} and \mathbf{R} are the relative and center-of-mass coordinate of the two interacting nucleons and where the values of the force parameters t_i , x_j , and α differ from one Skyrme interaction to another.^{11,12} (For this demonstration the spin-orbit interaction has been neglected since it has very little influence on the proton-neutron potential and densities. The full Skyrme force including a spin-orbit interaction term was, however, used in all the calculations.) The corresponding Skyrme-HF potentials are given by

$$\begin{aligned} U_q(\mathbf{r}) = & t_0 \left[\left[1 + \frac{x_0}{2} \right] \rho - \left(\frac{1}{2} + x_0 \right) \rho_q \right] + \frac{1}{4} \left[t_1 \left[1 + \frac{x_1}{2} \right] + t_2 \left[1 + \frac{x_2}{2} \right] \right] \tau - \frac{1}{4} [t_1 \left(\frac{1}{2} + x_1 \right) - t_2 \left(\frac{1}{2} + x_2 \right)] \tau_q \\ & - \frac{1}{8} \left[3t_1 \left[1 + \frac{x_1}{2} \right] - t_2 \left[1 + \frac{x_2}{2} \right] \right] \nabla^2 \rho + \frac{1}{8} [3t_1 \left(\frac{1}{2} + x_1 \right) + t_2 \left(\frac{1}{2} + x_2 \right)] \nabla^2 \rho_q \\ & + \frac{t_3}{12} \left[\left[1 + \frac{x_3}{2} \right] (\alpha + 2) \rho^{\alpha+1} - \left(\frac{1}{2} + x_3 \right) [\alpha \rho^{\alpha-1} (\rho_n^2 + \rho_p^2) + 2\rho^\alpha \rho_q] \right], \quad q = \{n, p\}, \end{aligned} \quad (2)$$

where $\rho = \rho_n + \rho_p$ is the total density and where τ_n and τ_p are the neutron and proton kinetic energy density. The difference in the potentials is given by

$$\begin{aligned} U_1 = U_p - U_n = & -t_0 \left(\frac{1}{2} + x_0 \right) (\rho_p - \rho_n) - \frac{1}{4} [t_1 \left(\frac{1}{2} + x_1 \right) - t_2 \left(\frac{1}{2} + x_2 \right)] (\tau_p - \tau_n) \\ & + \frac{1}{8} [3t_1 \left(\frac{1}{2} + x_1 \right) + t_2 \left(\frac{1}{2} + x_2 \right)] (\nabla^2 \rho_p - \nabla^2 \rho_n) - \frac{t_3}{6} \left(\frac{1}{2} + x_3 \right) \rho^\alpha (\rho_p - \rho_n). \end{aligned} \quad (3)$$

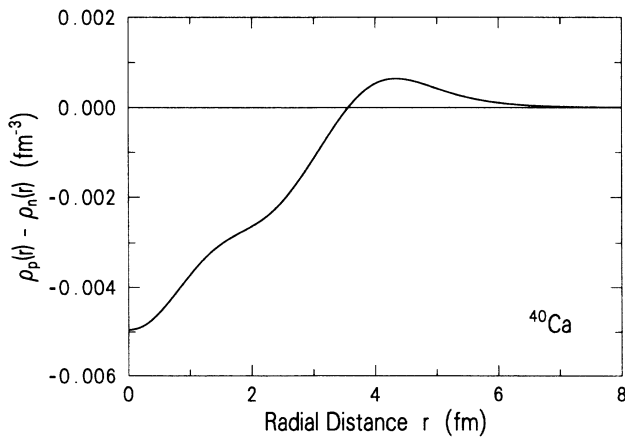


FIG. 1. Difference $\rho_p - \rho_n$ of the proton and neutron densities as a function of the radial distance obtained in a Hartree-Fock calculation with the Skyrme SIII force for the nucleus ^{40}Ca .

A numerical evaluation of this expression for ^{40}Ca is shown in Fig. 2. We see indeed that U_n is more attractive than U_p at the surface. The difference $U_p - U_n$ at its maximum ($r_m \approx 4.5$ fm) is about 2% of the average potential $U_0 \equiv \frac{1}{2}(U_p + U_n)$.

Sometimes these potentials are characterized in terms of their volume integral:

$$J = \int U(\mathbf{r}) d^3r. \quad (4)$$

For potential differences that have a node, however, this volume integral is not a very good characterization of the potential, especially when the projectile is a strongly absorbed probe. But even for probes that are not very strongly absorbed the use of a volume integral to characterize the potential might be misleading. For example, when the volume integral of U_1 in Eq. (3) is calculated the leading term will vanish for $N=Z$ nuclei since

$$\int [\rho_p(\mathbf{r}) - \rho_n(\mathbf{r})] d^3r = Z - N, \quad (5)$$

but also the contribution from the third term in Eq. (3)

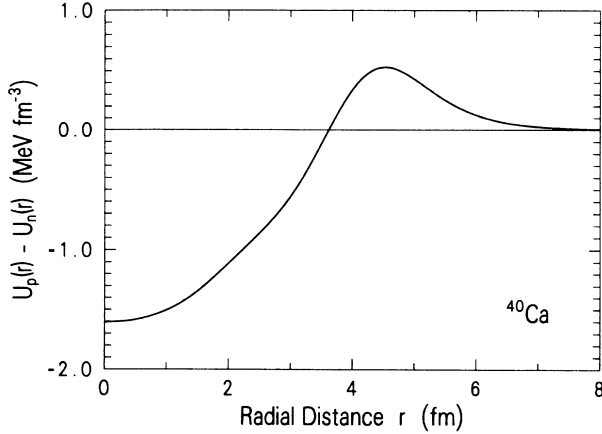


FIG. 2. Same as Fig. 1 but for the difference in the HF single-particle potentials $U_p(r) - U_n(r)$.

will vanish identically since the volume integral of the divergence of a vector field vanishing at infinity is zero.

For deformed nuclei, which are the main subject of this study, the densities and potentials can be characterized by their multipole decomposition which could be defined as

$$F^{(l)}(r) = \int F(\mathbf{r}) Y_l(\Omega) d\Omega, \quad (6)$$

where $Y_l(\Omega)$ is the spherical harmonic function of order l and the integration $d\Omega$ is over the angles. For example we may consider the quadrupole contribution of the potential

$$U^{(2)}(r) = \int U(\mathbf{r}) Y_2(\Omega) d\Omega. \quad (7)$$

Thus a comparison of $U_1^{(l)}$ and $U_0^{(l)}$ is one of the possible ways to characterize the charge-asymmetric potential resulting from core polarization by the Coulomb force in deformed $N = Z$ nuclei such as ^{28}Si or ^{32}S . For an axially symmetric nucleus one can define instead

$$\rho^{(l)}(r) = \frac{1}{2} \int_0^\pi \rho(r, \theta) P_l(\cos\theta) \sin\theta d\theta \quad (8)$$

and a corresponding expression for the potential $U^{(l)}(r)$

$$U^{(l)}(r) = \frac{1}{2} \int_0^\pi U(r, \theta) P_l(\cos\theta) \sin\theta d\theta. \quad (9)$$

For a spherical nucleus like ^{40}Ca , of course, only the monopole component ($l=0$) contributes.

We should mention that the core-polarization effect discussed here could be obtained in the case of bound states by performing a self-consistent calculation in the $A+1$ system. As it is well known such a self-consistent treatment can be presented as the coupling of the extra particle to the self-consistent ground and RPA excited states of the A particle system. So what we are presenting here is the charge-asymmetric aspect of such a coupling. In our case the relevant excitations would be the isovector monopole^{5,7,8} and because of the deformation in the considered nuclei also the quadrupole state.

There is also a very small charge asymmetric effect in the core-polarization process that has to do with the fact

that the extra proton and neutron have *slightly* different radial wave functions inside the nucleus. This correction should be present when actual optical model calculations are performed.

III. METHODS OF CALCULATION

Our main aim, as already mentioned, is to calculate the proton-neutron density and one-body (HF) potential differences in deformed nuclei, and to answer the question of whether deformation can lead to an enhancement in the difference of $\rho_p - \rho_n$ (or $U_p - U_n$) as compared with the case of spherical nuclei. The deformed nuclei we studied are the *sd*-shell nuclei ^{28}Si and ^{32}S . For the description of deformed *sd*-shell nuclei we have chosen the constrained Hartree-Fock (CHF) method with effective nucleon-nucleon interactions of the Skyrme type.^{11,12} Some of the most successful of these forces not only reproduce very precisely the total binding energy of spherical as well as deformed nuclei throughout the Periodic Table, but also describe very accurately the nuclear shape, its surface diffuseness and deformation. This is not only evident by the reproduction in Skyrme HF calculations of nuclear charge densities and cross sections for elastic electron scattering,^{11,12} but also by the accurate description of charge rms radii and measured multipole moments from *sd*-shell nuclei^{13,14} to the strongly deformed nuclei of the rare-earth region,^{15,16} and even to the very large deformations encountered in the fission process of actinides.^{17,18} The advantage of this method over other more phenomenological approaches is given by the fact that these calculations are based on a variational principle and are self-consistent, being all carried out with the same effective interaction with no additional parameters.

For deformed nuclei like those encountered in the fission process, in the rare-earth region and also in the *sd* shell, a mean-field calculation which constrains the nuclear shape has to be carried out. To describe such a deformed nucleus, CHF calculations with a constraint on one or a few collective variables are usually performed. In determining the nuclear structure of the deformed *sd*-shell nuclei ^{28}Si and ^{32}S investigated here, a quadratic constraint was used which was limited to the mass quadrupole moment, as done in most CHF calculations. The stationary points of the deformation energy curve¹⁹ like the ground state or shape isomeric states, if present, are correctly obtained in this way. Constraints on more than one multipole moment can, however, be relevant if the dynamical deformation path is to be described. Let us mention here that the deformed *sd*-shell nuclei show, in fact, secondary minima which are oblate for the prolate ground-state nuclei ^{20}Ne , ^{24}Mg , ^{32}S , and prolate secondary minima appear for the oblate ground-state nuclei ^{26}Si and ^{36}Ar .²⁰

In solving the Skyrme Hartree-Fock equations one can take advantage of the following symmetries. We impose axial symmetry on the solutions of the HF equations which for the deformed nuclei ^{28}Si and ^{32}S considered here is a very reasonable assumption. Taking the symmetry axis to be the z axis means that the Hartree-Fock

SP state i is eigenstate of the third component J_z of the total angular momentum with eigenvalue Ω_i , and of the third component τ_z of the isospin operator with eigenvalues $q_i = \frac{1}{2}$ for protons, $-\frac{1}{2}$ for neutrons. Since the state i and its time reversed state \bar{i} contribute equally to the local density $\rho(\mathbf{r})$, the kinetic energy density $\tau(\mathbf{r})$ and the spin-orbit density $\mathbf{J}(\mathbf{r})$, which enter the Skyrme Hamiltonian, it is sufficient to consider only positive values of Ω . Restricting ourselves to reflection symmetric shapes (left-right symmetry) results in the parity to be a good quantum number. The HF single-particle states are thus characterized by Ω^π .

To calculate nuclear deformation-energy surfaces, the CHF equations are solved, for the imposed symmetries (axial and left-right symmetry), by expanding the single-particle wave functions in eigenstates of an axially deformed harmonic oscillator,^{21,19} which in cylindrical coordinates $[z, \xi = (x^2 + y^2)^{1/2}, \phi]$ is written as

$$V_{\text{HO}}(\mathbf{r}) = \frac{m}{2}(\omega_z^2 z^2 + \omega_\xi^2 \xi^2). \quad (10)$$

Its eigenstates can be characterized by the number of nodes n_z and n_ξ in z and ξ direction and by the projections Λ and Σ of the orbital angular momentum and of the spin on the z axis. Characterizing a set of these quantum numbers by α it can be shown¹⁹ that the matrix $H_{\alpha\beta}$ of the HF Hamiltonian is block diagonal, each block being characterized by $\Omega = \Lambda + \Sigma$ and the parity $\pi = (-1)^{n_z + \Lambda}$.

Such an expansion necessarily involves a truncation of the basis and attention has to be paid to the convergence of this expansion.²² The oscillator parameters ω_z and ω_ξ are determined by minimizing the total energy with respect to these parameters for every given deformation, as defined for example by the mass quadrupole moment.

As mentioned above, one has to correct the deformation energy curve obtained in this way for the effect of an expansion in a finite basis. This truncation-energy correction can be easily obtained for a spherical shape where the HF equations can be directly solved in coordinate space. We assume that this truncation effect is deformation independent, which is a good approximation as long as the SP basis is not chosen too small and not too strongly necked-in nuclear shapes are to be considered. For the small deformations encountered in sd -shell nuclei and the large basis used in our calculation (7 or 9 major shells corresponding to 84, respectively, 165 single-particle states for a spherical shape) these limitations do not apply.

In these calculations the direct Coulomb energy is calculated exactly whereas the exchange contribution is included in the Slater approximation.^{23,24} The spurious center-of-mass motion inherent in any mean-field approach has been corrected for its one-body part only, the two-body part being neglected. As the parameters of the Skyrme force SIII (Ref. 10) used in the calculations presented here have been adjusted using exactly these approximations, this procedure seems the most adequate to us.

Pairing correlations have not been included in our calculations of deformed sd -shell nuclei, similar to previous calculations.^{13,14,20} Pairing effects should, however, be taken into account since the level density around the Fermi surface is substantially larger for these than for the neighboring spherical nuclei ^{16}O and ^{40}Ca . We have tried to carry out a full HF + BCS (Bardeen-Cooper-Schrieffer) calculation for these nuclei with a constant pairing strength G , which was determined at each deformation (and, in fact, at each iteration of the HF cycle) by solving the gap equation for the average level distribution obtained through a Strutinsky smoothing procedure,²⁵ the so called "uniform gap method."²⁶ This resulted, however, in a very large pairing strength leading to spherical solutions. Our understanding of this fact is that the approximation of a constant pairing strength is not applicable for these light nuclei and that the pairing matrix elements should be calculated explicitly. With very few exceptions,^{27,28} the correct description of pairing properties has, however, not entered the process of adjusting the different Skyrme-force parametrizations. As the pairing properties are treated anyhow in a HF + BCS approach, described above, as additional parameters (in the above-mentioned uniform gap method the additional parameter is the average pairing gap $\bar{\Delta} = 12 \text{ MeV}/\sqrt{A}$), one could also use, for the inclusion of pairing correlations, a finite-range effective interaction, like the Gogny force,²⁹ which has been explicitly constructed to have correct pairing properties.

The nucleus ^{40}Ca was treated as spherical and the HF calculation was performed using the spherical HF code. For consistency reasons the deformed code was also employed for ^{40}Ca imposing zero deformation. The two calculations gave very similar numerical results for the ^{40}Ca HF densities and potentials, indicating that convergence has been obtained in the expansion of the HF single-particle states in a finite basis.

IV. RESULTS AND CONCLUSIONS

The CHF calculations of the two sd -shell nuclei ^{28}Si and ^{32}S lead to rather shallow minima around the ground-state deformation corresponding to quadrupole moments $Q_2^{(n)} = -40.6 \text{ fm}^2$ and $Q_2^{(p)} = -41.7 \text{ fm}^2$ for the neutron and proton distribution in ^{28}Si , and $Q_2^{(n)} = 39.4 \text{ fm}^2$ and $Q_2^{(p)} = 40.8 \text{ fm}^2$ for ^{32}S . Thus, the ^{28}Si nucleus turns out to be a somewhat deformed oblate nucleus while ^{32}S is prolate. Note that there is a significant asymmetry of around 3% in the quadrupole moments of neutrons and protons in the two nuclei. For a better characterization of the ground states we give in Table I the charge rms radii, the quadrupole and hexadecapole moments of these nuclei and compare them to available experimental data. While the rms radii (in the calculation of the charge rms radii a Gaussian proton charge form factor and the standard center-of-mass correction³⁰ $\Delta r = -1.1 \text{ fm}/A$ have been included) are in excellent agreement with the experimental data, the calculated quadrupole moments are consistently too small^{13,20} and account only for about 70% of the experimental moments, obtained from measured $B(E2)$ values.

TABLE I. Charge rms radius, quadrupole moment $Q_2 = 2 \int r^2 P_2(\cos\theta) \rho(r) d^3r$, and hexadecapole moment $Q_4 = 2 \int r^4 P_4(\cos\theta) \rho(r) d^3r$ for the deformed ground states of ^{28}Si and ^{32}S obtained in a constrained HF approach with the Skyrme force SIII as compared to experimental data.

		HF SIII	Exp.
^{28}Si	r_c (fm)	3.14	3.14 ^a 3.09±0.02 ^b
	Q_2 (fm ²)	-41.7	-57.7±1.0 ^c
	Q_4 (fm ⁴)	137.4	
^{32}S	r_c (fm)	3.25	3.24±0.2 ^b
	Q_2 (fm ²)	40.8	54.9±1.2 ^c
	Q_4 (fm ⁴)	-29.3	

^aY. Horikawa *et al.*, Phys. Lett. **36B**, 9 (1971).

^bC. S. Wu and L. Willets, Ann. Rev. Nucl. Sci. **19**, 546 (1969).

^cD. Schwalm, E. K. Warburton, and J. W. Olness, Nucl. Phys. **A293**, 425 (1977).

In Figs. 3 and 4 we present the monopole component of the density differences $\rho_p^{(0)}(r) - \rho_n^{(0)}(r)$ and of the average density $\frac{1}{2}(\rho_p^{(0)} + \rho_n^{(0)})$ for ^{28}Si and ^{32}S [the difference $\rho_p(r) - \rho_n(r)$ for ^{40}Ca calculated using the spherical HF code was shown in Fig. 1]. In Fig. 5 the monopole components of the difference in the HF potential $U_p^{(0)}(r) - U_n^{(0)}(r)$ and of $U_0^{(0)}(r)$ are shown for ^{28}Si and in Fig. 6 for ^{32}S . For these two nuclei we also show in Fig. 7 the quadrupole contribution of the potential, $U_p^{(2)}(r) - U_n^{(2)}(r)$, as defined in Eq. (9).

As seen from the above figures the difference of the densities $\rho_1^{(0)}(r) = \rho_p^{(0)}(r) - \rho_n^{(0)}(r)$ in the surface (defined, e.g., by the 90–10% fall off) amounts to about 3–5% of the average density $\frac{1}{2}(\rho_p^{(0)} + \rho_n^{(0)})$. (It even becomes much bigger, of the order of 30%, in the far surface where the density falls off exponentially.) The same applies also to the inside part of the density, however, the sign of $\rho_1^{(0)}(r)$ is reversed. The same features appear also in the potentials. The difference $U_p^{(0)} - U_n^{(0)}$ is equal in the surface region to about 3–4% of the average potential $\frac{1}{2}(U_p^{(0)} + U_n^{(0)})$. The same is true in the case of ^{28}Si and ^{32}S for

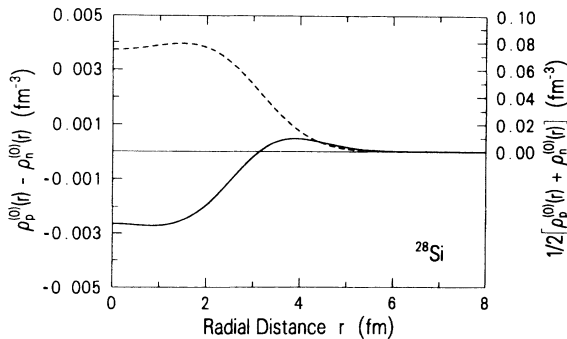


FIG. 3. Monopole part of the difference in the proton and neutron densities $\rho_p^{(0)}(r) - \rho_n^{(0)}(r)$ (solid line) and of the average density $\frac{1}{2}(\rho_p^{(0)} + \rho_n^{(0)})$ (dashed line) for the nucleus ^{28}Si .

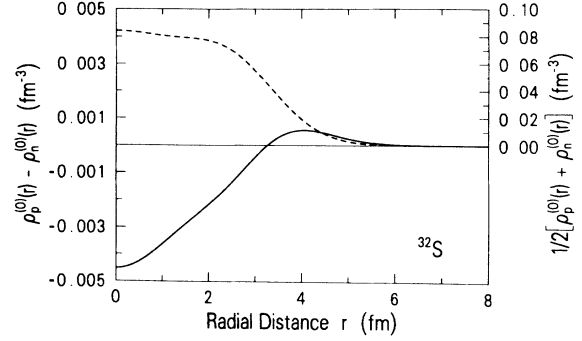


FIG. 4. Same as Fig. 3 but for the nucleus ^{32}S .

the $l=2$ components of the potential. That is, the size of $U_p^{(2)} - U_n^{(2)}$ in the surface region is several percent of the quadrupole contribution of the average potential $U_0^{(2)}$.

We should point out, however, that when the volume integrals of the potentials are calculated one finds that the difference of the proton-neutron volume integrals is only 0.5–1% that of the corresponding volume integral of the average potential. This is true in the case of the deformed nuclei ^{28}Si and ^{32}S as well as for the spherical ^{40}Ca . The reason is that, as already pointed out, there is a large cancellation taking place in the volume integrals and that, at least in the framework of Skyrme forces, the leading term, which is linear in the density, vanishes completely in the case of $N=Z$ nuclei when its volume integral is computed. One should expect therefore that for weakly distorted projectiles this charge-asymmetric potential will affect the cross section only a little leading to a 0.5–1% effect. However, for particles that experience stronger distortion effects and are absorbed at the surface, the calculated charge-asymmetric potential should lead to 3–5% asymmetries in the cross sections.

To make sure that our conclusions do not depend on the particular choice of the effective interaction used, the Skyrme force SIII in our case, we have performed the same calculations with a more recent Skyrme force, the

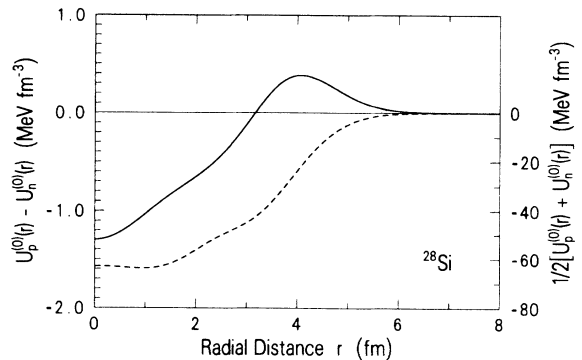
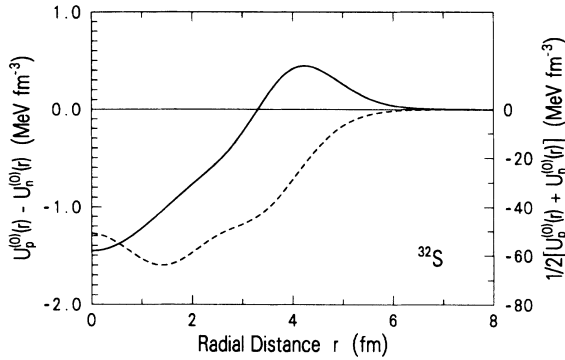


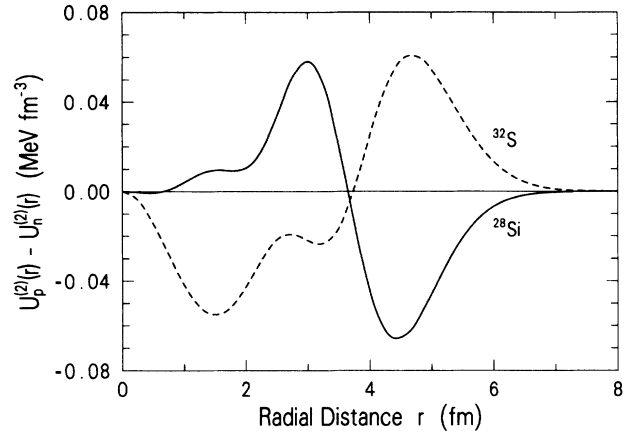
FIG. 5. Monopole part of the charge asymmetry potential $U_1 = U_p - U_n$ (solid line) and of the average potential $U_0 = \frac{1}{2}(U_p + U_n)$ (dashed line) for ^{28}Si .

FIG. 6. Same as Fig. 5 for the nucleus ^{32}S .

SkM^* (Refs. 18 and 31) interaction. The conclusions reached with this force are the same as those obtained with SIII. The ground states are very well reproduced as far as binding energies and charge rms radii are concerned, but the magnitude of the quadrupole moments are underestimated in deformed sd -shell nuclei. The core-polarization effects are large and of the same size as those found with SIII and a large cancellation takes place when volume integrals of the charge-asymmetry potentials are calculated.

We have also studied the question of whether the tendency of nuclei to become deformed (such as the ones in the middle of the sd shell) enhances the charge-asymmetry potential. The spherical solutions of the potentials U_p and U_n in ^{28}Si and ^{32}S were calculated and compared with the ground-state solutions. The deformation did not produce larger U_p, U_n asymmetries than in the corresponding spherical case. Thus, the core-polarization correction in deformed nuclei is not significantly larger than in spherical nuclei.

However, we should stress again that the charge-

FIG. 7. Quadrupole part of the charge-asymmetry potential $U_1 = U_p - U_n$ for the oblate nucleus ^{28}Si (solid line) and the prolate nucleus ^{32}S (dashed line).

symmetric core-polarization potentials in ^{28}Si , ^{32}S , and ^{40}Ca are large, of the order of several percent of the corresponding charge-symmetric potentials in the nuclear surface.

Whether these difference can account for the asymmetries found in proton and neutron scattering on these $N=Z$ nuclei can be answered after a detailed reaction calculation is performed in which the calculated HF potentials are taken as the real parts of the optical potential.

ACKNOWLEDGMENTS

We wish to thank Nguyen van Giai and P. Quentin for helpful discussions. One of us (J.B.) gratefully acknowledges a Feodor-Lynen Fellowship of the Alexander von Humboldt-Stiftung. This work was supported by the U.S. Department of Energy.

¹R. P. De Vito, S. M. Austin, W. Sterrenberg, and U. E. P. Berg, Phys. Rev. Lett. **47**, 628 (1981).

²J. S. Winfield *et al.*, Phys. Rev. C **33**, 1 (1986).

³J. S. Winfield, S. M. Austin, and B. A. Brown, Phys. Lett. B **196**, 311 (1987).

⁴R. Alarcon, J. Rapaport, and R. W. Finlay, Nucl. Phys. A **462**, 413 (1987).

⁵N. Auerbach, Phys. Rep. **98**, 273 (1983).

⁶J. A. Nolen and J. P. Schiffer, Annu. Rev. Nucl. Sci. **19**, 471 (1969).

⁷E. H. Auerbach, S. Kahana, and J. Weneser, Phys. Rev. Lett. **23**, 1253 (1969).

⁸N. Auerbach, Nucl. Phys. A **229**, 442 (1974).

⁹N. Auerbach and Nguyen van Giai, Phys. Rev. C **24**, 782 (1981).

¹⁰M. Beiner, H. Flocard, Nguyen van Giai, and P. Quentin, Nucl. Phys. A **283**, 29 (1975).

¹¹D. Vautherin and D. M. Brink, Phys. Rev. C **5**, 626 (1972).

¹²J. M. Giannoni and P. Quentin, Phys. Rev. C **21**, 2076 (1980).

¹³P. Quentin, Ph.D. thesis, Orsay, 1975.

¹⁴P. Quentin and H. Flocard, Annu. Rev. Nucl. Part. Sci. **28**, 523 (1978).

¹⁵H. Flocard, P. Quentin, and D. Vautherin, Phys. Lett. **46B**, 304 (1973).

¹⁶J. Bartel, M. B. Johnson, and M. Singham (unpublished).

¹⁷H. Flocard, P. Quentin, D. Vautherin, M. Veneroni, and A. K. Kerman, Nucl. Phys. A **231**, 176 (1974).

¹⁸J. Bartel, P. Quentin, M. Brack, C. Guet, and H.-B. Håkansson, Nucl. Phys. A **386**, 79 (1982).

¹⁹D. Vautherin, Phys. Rev. C **7**, 296 (1973).

²⁰P. Quentin, in *Nuclear Selfconsistent Fields*, edited by G. Ripka and M. Porneuf (North-Holland, Amsterdam, 1975), p. 297.

²¹J. Damgaard, H.-C. Pauli, V. V. Pashkevich, and V. M. Strutinsky, Nucl. Phys. A **135**, 432 (1969).

²²H. Flocard, P. Quentin, A. K. Kerman, and D. Vautherin, Nucl. Phys. A **203**, 433 (1973).

²³J. C. Slater, Phys. Rev. **81**, 85 (1951).

- ²⁴J. W. Negele and D. Vautherin, *Phys. Rev. C* **5**, 1472 (1972).
²⁵V. M. Strutinsky, *Nucl. Phys.* **A122**, 1 (1968).
²⁶M. Brack *et al.*, *Rev. Mod. Phys.* **44**, 320 (1972).
²⁷M. Waroquier, K. Heyde, and G. Wenes, *Nucl. Phys.* **A404**, 269 (1983).
²⁸J. Dobaczewski, H. Flocard, and J. Treiner, *Nucl. Phys.* **A422**, 103 (1984).
²⁹J. Dechargé and D. Gogny, *Phys. Rev. C* **21**, 1568 (1980).
³⁰J. W. Negele, *Phys. Rev. C* **1**, 1260 (1970).
³¹M. Brack, C. Guet, and H.-B. Håkansson, *Phys. Rep.* **123**, 275 (1985).